ICES Journal of Marine Science

ICES Journal of Marine Science (2018), doi:10.1093/icesjms/fsx239

Diatom performance in a future ocean: interactions between nitrogen limitation, temperature, and CO_2-induced seawater acidification

Futian Li[1], John Beardall[1,2], and Kunshan Gao[1]*

[1]*State Key Laboratory of Marine Environmental Science/Department of Marine Biological Science & Technology, College of Ocean and Earth Sciences, Xiamen University, Xiang'an South Road, Xiamen 361102, China*
[2]*School of Biological Sciences, Monash University, Wellington Road, Clayton, Victoria 3800, Australia*

**Corresponding author: tel: +86 592 2187982; fax: +86 592 2187963; e-mail: ksgao@xmu.edu.cn*

Li, F., Beardall, J., and Gao, K. Diatom performance in a future ocean: interactions between nitrogen limitation, temperature, and CO_2-induced seawater acidification. – ICES Journal of Marine Science, doi:10.1093/icesjms/fsx239.

Received 12 June 2017; revised 24 November 2017; accepted 12 December 2017.

Phytoplankton cells living in the surface waters of oceans are experiencing alterations in environmental conditions associated with global change. Given their importance in global primary productivity, it is of considerable concern to know how these organisms will perform physiologically under the changing levels of pH, temperatures, and nutrients predicted for future oceanic ecosystems. Here we show that the model diatom, *Thalassiosira pseudonana*, when grown at different temperatures (20 or 24 °C), pCO_2 (400 or 1000 µatm), and nitrate concentrations (2.5 or 102.5 µmol l^{-1}), displayed contrasting performance in its physiology. Elevated pCO_2 (and hence seawater acidification) under the nitrate-limited conditions led to decreases in specific growth rate, cell size, pigment content, photochemical quantum yield of PSII, and photosynthetic carbon fixation. Furthermore, increasing the temperature exacerbated the negative effects of the seawater acidification associated with elevated pCO_2 on specific growth rate and chlorophyll content under the N-limited conditions. These results imply that a reduced upward transport of nutrients due to enhanced stratification associated with ocean warming might act synergistically to reduce growth and carbon fixation by diatoms under progressive ocean acidification, with important ramifications for ocean productivity and the strength of the biological CO_2 pump.

Keywords: CO_2, diatom, growth, nitrogen availability, photosynthesis, phytoplankton, temperature, *Thalassiosira pseudonana*.

Introduction

Increasing emissions of anthropogenic carbon dioxide (CO_2) result in global warming that leads to increases in sea surface temperatures (ocean warming). While continuous dissolution of CO_2 into oceans remediates atmospheric CO_2 increases and global warming, it also leads to ocean acidification (Gattuso *et al.*, 2015). Average global ocean pH has already declined by 0.1 units since the Industrial Revolution and is predicted to further drop by up to 0.4 units by the end of this century (Gattuso *et al.*, 2015). Both ocean warming and acidification affect the availability of nitrogen and other nutrients to phytoplankton living in the surface layers of the ocean. Intensified stratification of surface waters caused by ocean warming decreases upward transport of nutrients across the thermocline (Rost *et al.*, 2008; Beardall *et al.*, 2009; Gao *et al.*, 2012a) leading to reduced nutrient supply. Moreover, ocean acidification could decrease nitrification and thus the supply of oxidized nitrogen in the surface ocean (Beman *et al.*, 2011). These changes are expected to have far-reaching consequences for marine primary production and ecosystem sustainability and services (Gattuso *et al.*, 2015; Boyd *et al.*, 2016).

Seawater acidification treatment has been shown, in a range of microalgal species, to cause down-regulation of the energy-costly CO_2 concentrating mechanisms (CCMs) (Raven and Beardall, 2014 and references therein) and to reduce the intracellular dissolved inorganic carbon pool within phytoplankton cells (Liu *et al.*, 2017). It also decreases intracellular pH (Suffrian *et al.*, 2011) and increases the energy expenditure of the cells in maintaining cellular pH homeostasis (Taylor *et al.*, 2012). While the

physiological responses of phytoplankton to seawater acidification might vary between genera, species (Langer *et al.*, 2006; King *et al.*, 2015; Li *et al.*, 2016), and even among strains (Langer *et al.*, 2009), interactions with other environmental stressors can alter the responses to acidification (Li *et al.*, 2012a; Beardall *et al.*, 2014; Verspagen *et al.*, 2014; Passow and Laws, 2015; Li *et al.*, 2017a). In addition, the duration of growth under seawater acidification could also affect the physiological performance of phytoplankton cells due to acclimation and adaptation processes (Collins *et al.*, 2014; Li *et al.*, 2017b). Therefore, it is important to examine the effects of elevated CO_2 under changing environmental conditions or under multiple stressors in both the short and the long term. Interactions between acidification and other factors, such as light intensity (Gao *et al.*, 2012b; Li *et al.*, 2014; Heiden *et al.*, 2016), light fluctuation (Hoppe *et al.*, 2015), solar UV radiation (Li *et al.*, 2012a), temperature (Torstensson *et al.*, 2012; Torstensson *et al.*, 2013; Coello-Camba *et al.*, 2014), and availability of iron (Sugie and Yoshimura, 2013, 2016; Segovia *et al.*, 2017) and other nutrients (King *et al.*, 2011; Sun *et al.*, 2011; Li *et al.*, 2012b) have been reported in diatoms.

Diatoms are responsible for about 40% of oceanic primary production and account for over 50% of organic carbon burial in marine sediments (Falkowski *et al.*, 2004). Hence, the responses of their growth and photosynthesis to changing marine environments are likely to influence the export of organic matter to deep water and the biogeochemical cycling of carbon, silicon, and other elements. For instance, diatoms dominate the open ocean microphytoplankton community and live cells have been found in the deep ocean (down to 4000 m), indicating their critical role in the biological CO_2 pump (Agusti *et al.*, 2015). On the other hand, N-limitation is usually exacerbated by higher half-saturation constants for nitrate uptake of diatoms compared to other algal classes (Eppley *et al.*, 1969; Falkowski, 1975; Moore *et al.*, 2002a). Indeed, about 50% of surface oceans are nitrogen-limited for diatoms, at least, during summer (Moore *et al.*, 2002b). Given the decreased upward transport of nutrients, decreasing nitrification, and higher half-saturation constants for nitrate uptake, diatoms within the upper mixed layers will become especially exposed to increasing nutrient limitation under the influences of ocean warming and acidification.

However, few studies have investigated combined effects among elevated CO_2, temperature, and nutrient limitation (Taucher *et al.*, 2015), in part because of the complexity of interactive effects (Boyd *et al.*, 2016). In terms of CO_2 and temperature interactions, growth rates of several diatom species freshly isolated from coastal New Zealand waters have been shown to be enhanced, depressed, or unaltered by elevated temperature and CO_2, with temperature showing more prominent effects than CO_2 (Tatters *et al.*, 2013). In contrast, growth of *Chaetoceros cf. wighamii* was mainly affected by elevated CO_2, rather than by the temperature levels tested (Araújo and Garcia, 2005). On the other hand, elevated levels of temperature and CO_2 synergistically enhanced the growth of the Antarctic diatom *Nitzschia lecointei* (Torstensson *et al.*, 2013), but depressed the primary production of Arctic phytoplankton (Coello-Camba *et al.*, 2014), showing that phytoplankton may show different regional responses. In another study, however, seawater acidification treatment substantially enhanced the growth of diatoms in a phytoplankton community, whereas their growth was unaltered when CO_2 and temperature were both elevated (Feng *et al.*, 2009). Effects of elevated CO_2 and associated seawater acidification on diatoms have been extensively studied under nitrogen-replete conditions (Gao and Campbell, 2014 and references therein). However, it has been suggested that the effects of acidification might differ under nutrient-limited compared to replete conditions (Taucher *et al.*, 2015). For instance, the carbon to nitrogen ratios in *Phaeodactylum tricornutum*, *Thalassiosira pseudonana*, and *Thalassiosira weissflogii* were raised by acidification treatment only under N-limited conditions (Li *et al.*, 2012b; Hong *et al.*, 2017). Additionally, seawater acidification only increased photosynthetic carbon fixation and maximum relative electron transport of *P. tricornutum* when nitrogen availability was sufficient (Li *et al.*, 2012b; Hong *et al.*, 2017). There are also reports showing differential responses of diatoms to temperature changes grown at different concentrations of nutrients (Hagerthey *et al.*, 2002; Doyle *et al.*, 2005). While elevated temperature decreased the relative abundance of *Nitzschia frustulum* more conspicuously under low-nutrient conditions (Hagerthey *et al.*, 2002), it increased the growth of two other diatom species greatly when nutrients were added (Doyle *et al.*, 2005).

As a much studied model diatom species, growth and photosynthesis of *T. pseudonana* have been shown to benefit from, or be unaltered by, seawater acidification (Sobrino *et al.*, 2008; Trimborn *et al.*, 2009; Crawfurd *et al.*, 2011; Gao *et al.*, 2012b; McCarthy *et al.*, 2012; Yang and Gao, 2012; Shi *et al.*, 2015; Hong *et al.*, 2017). However, acidification showed negative effects on photosynthesis when *T. pseudonana* was cultured in a nitrate-limited chemostat (similar growth rates of ambient and elevated CO_2 acclimated cells were controlled by the dilution rate and acidification effects were only studied under nitrate-limited conditions) (Hennon *et al.*, 2014). Changes in temperature and the availability of nitrate may alter the response of diatoms to elevated CO_2, as these changes would impact carbon and nitrogen metabolism and cellular energy budgets. We hypothesize that nitrate limitation may aggravate impacts of seawater acidification and superimposition of a warming treatment may further complicate the effects due to increased respiratory carbon loss under acidification and warming. In the present work, we tested this hypothesis by growing the diatom, *T. pseudonana*, under different levels of nitrate in combination with pCO_2 and temperature treatments.

Material and methods

Culture conditions and experimental design

The diatom *T. pseudonana* (CCMP 1335), originally isolated from coastal waters of Long Island (USA), was grown in 500 ml polycarbonate (PC) bottles maintained at 20 (LT) or 24 °C (HT) with a 12:12 h light–dark cycle. The temperatures were set according to the isolation temperature (20 °C), and the temperature rise of 4 °C was based on the RCP8.5 scenario that predicts the sea surface temperature will increase by this extent at the end of the 21st century (Bopp *et al.*, 2013). In addition, the two temperature regimes are near or in the optimal temperature range of this strain (Boyd *et al.*, 2013). The PC bottles were acid-cleaned and rinsed thoroughly with ultrapure water and autoclaved before being used for cell cultures. Photosynthetically active radiation (PAR) was set at 105 ± 6 µmol photons $m^{-2} s^{-1}$ (measured by a US-SQS/WB spherical micro quantum sensor; Walz), with no differences among positions where bottles were placed. The culture media were prepared with autoclaved artificial seawater with nutrients added according to the Aquil medium recipe (Sunda

Table 1. Experimental treatments and carbonate chemistry parameters of culture media.

Treatments	Temperature (°C)	Nitrate concentration (μmol l^{-1})	pCO_2 (μatm)	pH_{NBS}	TA (μmol kg^{-1})	DIC (μmol kg^{-1})	HCO_3^- (μmol kg^{-1})	CO_2 (μmol kg^{-1})
LTHNLC	20	102.5	400	8.11 ± 0.03	2274 ± 20	2024 ± 6	1836 ± 8	15 ± 1
LTHNHC	20	102.5	1000	7.81 ± 0.03*	2272 ± 28	2155 ± 17*	2026 ± 13*	33 ± 2*
LTLNLC	20	2.5	400	8.11 ± 0.02	2285 ± 20	2033 ± 8	1843 ± 1	15 ± 1
LTLNHC	20	2.5	1000	7.81 ± 0.02*	2298 ± 14	2181 ± 21*	2050 ± 22*	34 ± 2*
HTHNLC	24	102.5	400	8.11 ± 0.03	2269 ± 32	1991 ± 33	1784 ± 35	14 ± 1
HTHNHC	24	102.5	1000	7.79 ± 0.01*	2273 ± 33	2143 ± 32*	2006 ± 30*	32 ± 1*
HTLNLC	24	2.5	400	8.10 ± 0.02	2284 ± 15	2008 ± 10	1802 ± 13	14 ± 1
HTLNHC	24	2.5	1000	7.82 ± 0.02*	2308 ± 18	2165 ± 22*	2022 ± 22*	30 ± 2*

Values of carbonate chemistry parameters are means ± *SD* of triplicate cultures ($n = 3$). Asterisks indicate significant ($p < 0.05$) differences between pCO_2 treatments (*t*-test).

et al., 2005), except for nitrate. The maximum cell concentration was controlled below 6×10^4 cells ml^{-1} by dilution with target-CO_2 equilibrated media every 24 h in order to maintain constant seawater carbonate chemistry without aeration. All the cultures were grown in one growth chamber to prevent any potential influence of factors besides the ones under test from biasing the results.

The nitrate concentration of the medium was set as 102.5 μmol l^{-1} for the high nitrogen (HN) treatment. It was set at 2.5 μmol l^{-1} for the low nitrogen (LN) treatment, a concentration that is limiting to the diatom's growth (Li *et al.*, 2012b; Hennon *et al.*, 2014). The culture media were pre-aerated with low (~400 μatm, LC) or high pCO_2 (~1000 μatm, HC) air for about 24 h to ensure equilibration with the target pCO_2 levels. The CO_2-enriched air was achieved with a CO_2 plant growth chamber (HP1000G-D; Ruihua), in which the target pCO_2 levels were obtained by mixing air and pure CO_2 gas. Thus, eight treatments were achieved, and each treatment had three independent replicate cultures. All the culture bottles were placed randomly in the growth chamber to avoid artefacts related to inappropriate replication. Nitrate concentrations were determined by a nutrient autoanalyzer (AA3; Bran-Luebbe) in which nitrate was reduced to nitrite by cadmium. The lower detection limit of nitrate was 0.1 μmol l^{-1}. Nitrate concentrations dropped from 117.1 (±0.9) to 108.3 (±1.1) μmol l^{-1} in the HN cultures and from 2.4 (±0.1) to 0 μmol l^{-1} (under the limit of detection) in the LN cultures over the 24 h period, respectively. Cultures were run for at least 15 generations before physiological parameters were measured during the photoperiod (5–7 h after the onset of light).

Seawater carbonate chemistry

The pH_{NBS} was measured by a pH meter (Orion 2 STAR; Thermo Scientific) calibrated using standard National Bureau of Standards (NBS) buffers. Samples for total alkalinity (TA) measurement were poisoned by a saturated solution of mercuric chloride after filtering through cellulose acetate membranes (0.45 μm). TA was determined by Gran acidimetric titration on a 25-ml sample with a TA analyzer (AS-ALK1+; Apollo SciTech). Certified reference materials supplied by A. G. Dickson at the Scripps Institution of Oceanography were used to assure the accuracy of the TA measurement. Carbonate chemistry parameters were calculated based on the TA and pH values using the CO2SYS software, and are shown in Table 1.

Specific growth rate, cell size, and chlorophyll *a* content

Cell concentration and mean cell size were determined with 20 ml samples by a Coulter Particle Count and Size Analyzer (Z2; Beckman Coulter). Specific growth rate was calculated according to the equation: $\mu = (\ln N_1 - \ln N_0)/(t_1 - t_0)$, where N_1 and N_0 represent cell concentrations at t_1 (before dilution) and t_0 (initial or after dilution), $(t_1 - t_0) = 24$ h. Samples (150 ml) for chlorophyll measurement were filtered onto GF/F filters (25 mm; Whatman) and extracted in 5 ml of absolute methanol at 4 °C in darkness for 24 h. The supernatants obtained after centrifugation (5000 g for 10 min) were analysed by a UV-VIS Spectrophotometer (DU800; Beckman Coulter). The absorption values at 632, 665, and 750 nm were measured, and chlorophyll *a* concentrations were determined according to Ritchie (2006).

Biogenic silica and particulate organic carbon and nitrogen

Samples (120 ml) were gently filtered onto 1.2 μm PC filters (25 mm; Millipore) for determination of biogenic silica (BSi) according to Brzezinski and Nelson (1995). BSi on filters was digested by 4 ml of 0.2 mol l^{-1} NaOH for 45 min and neutralized with 1 ml of 1 mol l^{-1} HCl to terminate the extraction. The supernatants (1 ml) were then transferred to clean PE centrifuge plastic tubes (15 ml) and diluted with 4 ml of Milli-Q water. Ammonium molybdate (2 ml) and the reducing agent (3 ml) were added to the tubes and the absorption was measured at 810 nm by a UV-VIS Spectrophotometer (DU800; Beckman Coulter) within 2–3 h of extraction. Samples (100 ml) for measuring particulate organic carbon (POC) and nitrogen (PON) were harvested by gentle vacuum filtration (< 0.02 MPa) on pre-combusted (450 °C for 6 h) GF/F filters (25 mm; Whatman). HCl fumes were applied to remove any inorganic carbon on filters (12 h) before they were dried at 60 °C and analysed using a CHNS/O Analyzer (2400 SeriesII; PerkinElmer). Acetanilide of a known ratio of carbon to nitrogen and weight (range from 0.2 to 1 mg) was run every 6 samples to monitor instrument drift.

Chlorophyll *a* fluorescence

Samples were dark-adapted for 10 min before the maximum quantum yields of PSII ($\Phi_{PSII\ max}$) were measured with a multi-colour pulse amplitude modulated fluorometer (MULTI-COLOR-PAM; Walz). Preliminary experiments showed there was no difference between 10 and 15 min dark-adaptation times. Following dark-adaptation an actinic light of 94 μmol photons $m^{-2}\,s^{-1}$, being similar to the growth light level, was applied for 3 min to determine the effective quantum yield of PSII ($\Phi_{PSII\ eff}$).

The measuring beam and actinic light sources were blue and white light, respectively. The intensity of the saturating pulse was set at 4819 µmol photons $m^{-2} s^{-1}$ for 0.8 s. $\Phi_{PSII\ max}$ and $\Phi_{PSII\ eff}$ were calculated according to the following equations: $\Phi_{PSII\ max} = (F_m - F_0)/F_m$ for dark-adapted (10 min) samples; $\Phi_{PSII\ eff} = (F_m' - F_t)/F_m' = \Delta F/F_m'$ for actinic light-adapted samples, where F_m and F_m' indicate maximum chlorophyll fluorescence of dark- and light-adapted samples, respectively, F_0 is the minimum chlorophyll fluorescence of dark-treated cells, and F_t is the steady state chlorophyll fluorescence of the light-exposed samples. Rapid light curves (RLCs) were measured to estimate relative maximum electron transport rate ($rETR_{max}$), apparent photon transfer efficiency (α), and light saturation point (I_k). Samples were incubated under growth conditions (105 µmol photons $m^{-2} s^{-1}$; 20 and 24 °C for LT and HT treatments, respectively) for 10 min before RLC measurements. Eleven progressively increasing light intensities (60, 94, 128, 215, 368, 644, 798, 1149, 1599, 2120, and 2863 µmol photons $m^{-2} s^{-1}$), each applied for 20 s, were used in the RLC measurements. Values of rETR at these light intensities were calculated according to: $rETR = PAR \times \Phi_{PSII\ eff} \times 0.5$, where PAR represents the photon flux density of actinic light (µmol photons $m^{-2} s^{-1}$), $\Phi_{PSII\ eff}$ is the effective photochemical quantum yield at each PAR level, and the factor 0.5 assumes that PSII receives half of all absorbed quanta. PAR and rETR data obtained from RLCs were fitted to the model: $rETR = PAR/(a \times PAR^2 + b \times PAR + c)$. The I_k, $rETR_{max}$ and α were calculated from a, b and c according to Eilers and Peeters (1988).

Photosynthesis and dark respiration

Samples (20 ml) of cultures with a cell concentration range of 2–6 × 10^4 cells ml^{-1} were inoculated with 5 µCi $NaH^{14}CO_3$ (ICN Radiochemicals) for determination of photosynthetic carbon fixation rates. They were incubated under growth conditions (105 µmol photons $m^{-2} s^{-1}$, 20 or 24 °C) for 60 min. This relatively short-term incubation is usually taken to give an estimation of gross photosynthetic carbon fixation rate (Williams *et al.*, 2002), though some other studies have indicated that N status might influence the balance between gross and net carbon fixation (Halsey *et al.*, 2011, 2013). After the incubation, cells were gently filtered onto GF/F filters (25 mm; Whatman) and the filters were placed into scintillation vials. Filters were exposed to HCl fumes overnight, and dried at 50 °C for 6 h (Gao *et al.*, 2007). Scintillation cocktail (5 ml) was added to the vials before assimilated radiocarbon was counted by a liquid scintillation counter (Tri-Carb 2800TR; PerkinElmer).

Dark respiration was measured by a Clark-type oxygen electrode (Oxygraph; Hansatech). About 1 × 10^6 cells were harvested by gentle vacuum filtration (<0.02 MPa) onto cellulose acetate membranes (1 µm) and resuspended into 5 ml of 20 mmol l^{-1} Tris-buffered medium. Then they were injected into the oxygen electrode chamber at 20 or 24 °C controlled by a refrigerated circulating bath (GDH-0506; Shunma). $\Phi_{PSII\ max}$ was measured to ensure physiological stability after the influence of filtration; no differences were found in $\Phi_{PSII\ max}$ before and after the filtration. The pH values (8.10 and 7.80 for LC and HC conditions, respectively) of the Tris-buffered media were adjusted to the corresponding culture values by 1 mol l^{-1} HCl and NaOH. Dark respiration rates were derived from the linear portion of the slope of oxygen consumption vs. time (within about 10 min per measurement).

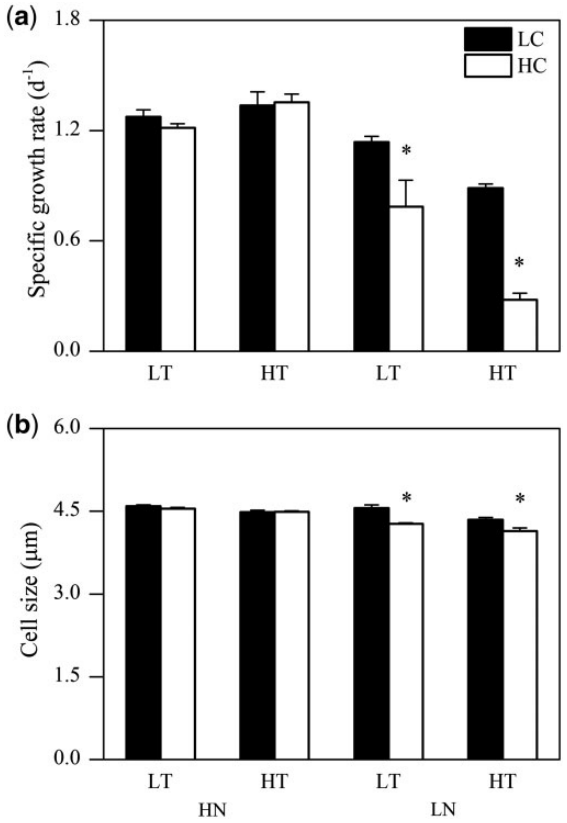

Figure 1. Specific growth rates (d^{-1}) (a) and cell size (µm) (b) of *Thalassiosira pseudonana* acclimated to ambient (LC, filled bars) and elevated pCO_2 (HC, open bars) at different temperature and nitrate levels. The data are mean ± *SD* values of triplicate cultures ($n = 3$). Asterisks indicate significant ($p < 0.05$) differences between pCO_2 treatments (*t*-test).

Statistical analyses

All data in the present study are reported as the mean ± *SD* ($n = 3$). Data were analysed by the general linear model (GLM) in SPSS statistics 18.0, with temperature, nitrate concentration, and pCO_2 level as three factors in the model. Two levels were set in each factor: 20 and 24 °C for temperature; 2.5 and 102.5 µmol l^{-1} for nitrate concentration; 400 and 1000 µatm for pCO_2 level. Interactions among three factors were included in the model. The independent-samples *t*-test was applied to determine differences between two levels of a factor when $p < 0.05$ was found in the model.

Results

Specific growth rate and mean cell size

While elevated pCO_2 showed no significant impact on growth in HN-grown cells, it significantly decreased the specific growth rate of LN-grown cultures (31%, *t*-test, $t = 4.1$, $df = 4$, $p = 0.014$ for low temperature; 68%, $t = 24.7$, $df = 4$, $p < 0.001$ for high temperature; Figure 1a). Specific growth rates were 11–79% lower under N-limited conditions than replete conditions (*t*-test, $t = 4.9$, $df = 4$, $p = 0.008$ for low temperature plus ambient pCO_2 treatment; $t = 5.1$, $df = 4$, $p = 0.007$ for low temperature plus elevated pCO_2 treatment; $t = 10.1$, $df = 4$, $p = 0.001$ for high temperature plus ambient pCO_2 treatment; $t = 32.6$, $df = 4$, $p < 0.001$ for high temperature plus

Table 2. $\Phi_{PSII\ max}$ and $\Phi_{PSII\ eff}$, α, $rETR_{max}$, and I_k (μmol photons $m^{-2}\ s^{-1}$) of *Thalassiosira pseudonana* cells under different treatments.

		$\Phi_{PSII\ max}$	$\Phi_{PSII\ eff}$	α	$rETR_{max}$	I_k
LT (20 °C)	HNLC	0.671 ± 0.008	0.582 ± 0.008	0.268 ± 0.005	119 ± 1	444 ± 13
	HNHC	0.668 ± 0.003	0.575 ± 0.004	0.266 ± 0.002	117 ± 4	439 ± 15
	LNLC	0.635 ± 0.016	0.549 ± 0.018	0.273 ± 0.010	97 ± 5	355 ± 32
	LNHC	0.538 ± 0.036*	0.488 ± 0.028*	0.239 ± 0.021	77 ± 5*	322 ± 8
HT (24 °C)	HNLC	0.678 ± 0.001	0.565 ± 0.005	0.277 ± 0.001	127 ± 1	458 ± 1
	HNHC	0.672 ± 0.003*	0.557 ± 0.006	0.273 ± 0.002*	117 ± 4*	430 ± 15
	LNLC	0.673 ± 0.004	0.593 ± 0.030	0.292 ± 0.002	109 ± 6	376 ± 21
	LNHC	0.505 ± 0.038*	0.472 ± 0.012*	0.221 ± 0.008*	75 ± 9*	341 ± 53

The data are means ± *SD* of triplicate cultures ($n = 3$). Asterisks indicate significant ($p < 0.05$) differences between pCO_2 treatments (*t*-test).
HNLC, high nitrate low pCO_2 treatment; HNHC, high nitrate high pCO_2 treatment; LNLC, low nitrate low pCO_2 treatment; LNHC, low nitrate high pCO_2 treatment.

Table 3. Significance test results for temperature (T), nitrate (N), pCO_2 (C), and their interactions based on the GLM.

Parameter	T		N		C		T × N		T × C		N × C		T × N × C	
	F	*p*	F	*p*	F	*p*	F	*p*	F	*p*	F	*p*	F	*p*
Specific growth rate	28.8	**<0.001**	406.3	**<0.001**	93.0	**<0.001**	85.5	**<0.001**	2.9	0.107	78.1	**<0.001**	10.2	**0.006**
Cell size	66.1	**<0.001**	166.2	**<0.001**	71.3	**<0.001**	8.0	**0.012**	4.4	0.052	53.0	**<0.001**	0.2	0.636
Chlorophyll *a*	0.3	0.559	432.6	**<0.001**	50.6	**<0.001**	82.3	**<0.001**	3.5	0.079	20.3	**<0.001**	0.01	0.907
BSi	3.0	0.100	0.5	0.492	0.4	0.504	0.01	0.898	0.4	0.520	7.2	**0.016**	2.8	0.109
POC	2.8	0.113	11.3	**0.004**	74.6	**<0.001**	6.3	**0.023**	9.7	**0.007**	77.1	**<0.001**	1.4	0.252
PON	58.5	**<0.001**	20.4	**<0.001**	85.4	**<0.001**	0.01	0.903	1.7	0.203	34.8	**<0.001**	5.1	**0.037**
C: N	70.1	**<0.001**	181.9	**<0.001**	0.1	0.688	32.0	**<0.001**	34.7	**<0.001**	13.9	**0.002**	23.7	**<0.001**
Si: C	5.2	**0.035**	0.1	0.706	94.8	**<0.001**	1.1	0.290	17.9	**0.001**	40.4	**<0.001**	6.4	**0.022**
Photosynthesis	7.4	**0.015**	780.6	**<0.001**	98.7	**<0.001**	61.2	**<0.001**	7.8	**0.013**	53.7	**<0.001**	10.6	**0.005**
Dark respiration	94.3	**<0.001**	73.1	**<0.001**	33.7	**<0.001**	31.8	**<0.001**	11.8	**0.003**	33.7	**<0.001**	16.2	**0.001**

Bold and underlined values show where there are significant effects.

elevated pCO_2 treatment). Elevated temperature decreased cell growth under the reduced nitrate condition by 22 and 65% at the ambient and elevated pCO_2 levels, respectively (*t*-test, $t = 11.5$, $df = 4$, $p < 0.001$ for ambient pCO_2 level; $t = 5.9$, $df = 4$, $p = 0.004$ for elevated pCO_2 level). A significant interaction was found between nitrate and pCO_2 levels effects on specific growth rate (GLM, $F_{1,16} = 78.1$, $p < 0.001$; Table 3).

Elevated pCO_2 decreased the cell size under N-limited conditions (6%, *t*-test, $t = 8.1$, $df = 4$, $p = 0.001$ for low temperature; 5%, $t = 4.8$, $df = 4$, $p = 0.008$ for high temperature; Figure 1b), but had no significant effect on the HN-grown cells. Nitrate limitation decreased cell size by 3–7% compared to the corresponding HN treatments, with the exception of the low temperature plus ambient pCO_2 treatment. Cells grown at the higher temperature had 1–5% smaller mean cell sizes than in the corresponding LT treatments (*t*-test, $t = 4.3$, $df = 4$, $p = 0.012$ for N-replete plus ambient pCO_2 treatment; $t = 3.5$, $df = 4$, $p = 0.024$ for N-replete plus elevated pCO_2 treatment; $t = 5.0$, $df = 4$, $p = 0.007$ for N-limited plus ambient pCO_2 treatment; $t = 3.6$, $df = 4$, $p = 0.021$ for N-limited plus elevated pCO_2 treatment). A significant interaction between nitrate and pCO_2 levels on cell size was detected (GLM, $F_{1,16} = 53.0$, $p < 0.001$).

Chlorophyll *a*, BSi, POC, and PON

Differential responses of chlorophyll *a* content to elevated pCO_2 were detected under N-limited compared to N-replete conditions: elevated pCO_2 showed no significant effect under HN conditions but resulted in decreased chlorophyll *a* under LN conditions (56%, *t*-test, $t = 10.3$, $df = 4$, $p < 0.001$ for low temperature; 70%, $t = 11.2$, $df = 4$, $p < 0.001$ for high temperature; Figure 2a). LN treatments resulted in 22–89% lower chlorophyll *a* content compared to HN treatments (*t*-test, $t = 4.3$, $df = 4$, $p = 0.012$ for low temperature plus ambient pCO_2 treatment; $t = 4.9$, $df = 4$, $p = 0.008$ for low temperature plus elevated pCO_2 treatment; $t = 24.4$, $df = 4$, $p < 0.001$ for high temperature plus ambient pCO_2 treatment; $t = 28.9$, $df = 4$, $p < 0.001$ for high temperature plus elevated pCO_2 treatment), and elevated temperature increased the difference between LN and HN treatments. While elevated temperature decreased chlorophyll *a* content under LN conditions, it enhanced the content under HN conditions (*t*-test, $t = -4.1$, $df = 4$, $p = 0.015$ for N-replete plus ambient pCO_2 treatment; $t = -3.1$, $df = 4$, $p = 0.036$ for N-replete plus elevated pCO_2 treatment; $t = 11.3$, $df = 4$, $p < 0.001$ for N-limited plus ambient pCO_2 treatment; $t = 6.5$, $df = 4$, $p = 0.003$ for N-limited plus elevated pCO_2 treatment). A significant interaction between nitrate and pCO_2 levels on chlorophyll *a* content was detected (GLM, $F_{1,16} = 20.3$, $p < 0.001$). No significant effects of the three factors on BSi content were found (Table 3), and cell quotas ranged from 0.09 to 0.13 pmol $cell^{-1}$ (Figure 2b).

Differential effects of elevated pCO_2 on POC content under LN and HN conditions were detected: pCO_2 had no significant impact under HN conditions, but increased POC content by 78–167% under LN conditions (*t*-test, $t = -4.2$, $df = 4$, $p = 0.013$ for low temperature; $t = -29.2$, $df = 4$, $p < 0.001$ for high temperature; Figure 2c). POC contents of LN cells were 24–28% lower than in the corresponding HN treatments at ambient pCO_2

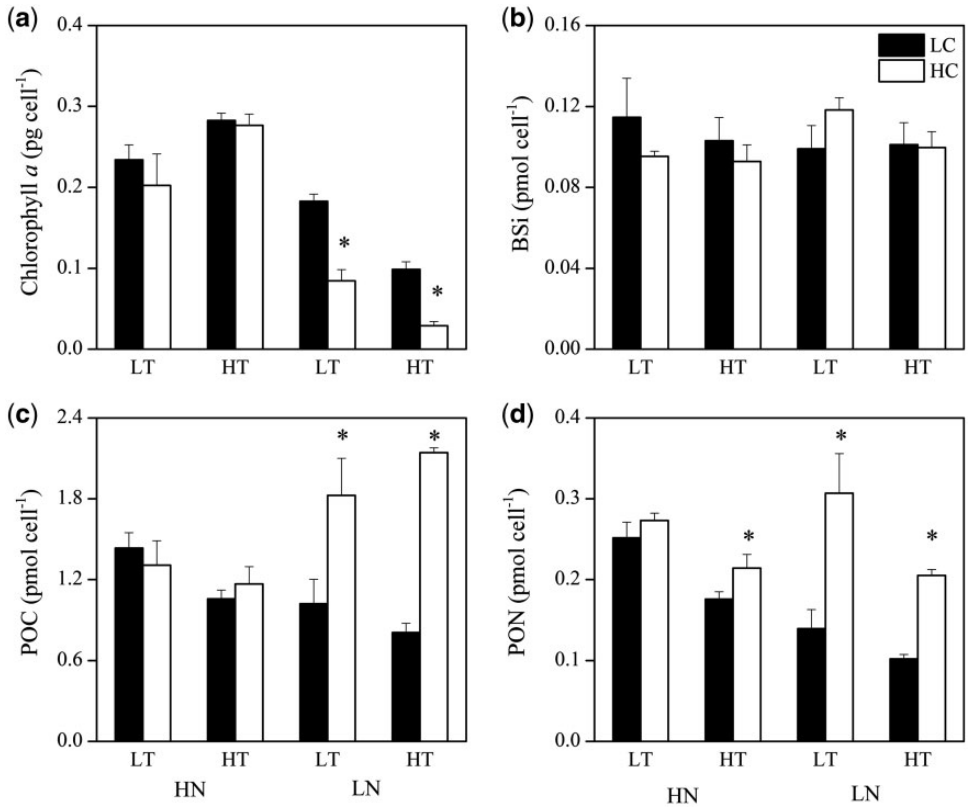

Figure 2. Cellular quotas of chlorophyll *a* (pg cell^{-1}) (a), BSi (pmol cell^{-1}) (b), POC (pmol cell^{-1}) (c), and PON (pmol cell^{-1}) (d) of *Thalassiosira pseudonana* acclimated to ambient (LC, filled bars) and elevated pCO_2 (HC, open bars) at different temperature and nitrate levels. The data are mean ± *SD* values of triplicate cultures ($n = 3$). Asterisks indicate significant ($p < 0.05$) differences between pCO_2 treatments (*t*-test).

(*t*-test, $t = 3.3$, $df = 4$, $p = 0.029$ for low temperature; $t = 4.5$, $df = 4$, $p = 0.010$ for high temperature), but POC was enhanced by nitrate limitation at elevated pCO_2. Temperature showed no significant effects on cellular POC content (GLM, $F_{1,16} = 2.8$, $p = 0.113$). Interactions between temperature or nitrate and pCO_2 levels on POC content were detected (Table 3).

Elevated pCO_2 significantly enhanced PON contents by 23–131% (*t*-test, $t = -3.4$, $df = 4$, $p = 0.026$ for low temperature plus N-limited treatment; $t = -5.3$, $df = 4$, $p = 0.006$ for high temperature plus N-replete treatment; $t = -20.0$, $df = 4$, $p < 0.001$ for high temperature plus N-limited treatment; Figure 2d), with the exception of the low temperature plus N-replete treatment. LN-grown cells showed 41–48% lower PON content relative to HN-grown cells under ambient pCO_2 conditions (*t*-test, $t = 6.3$, $df = 4$, $p = 0.003$ for low temperature; $t = 12.1$, $df = 4$, $p < 0.001$ for high temperature), but there was no difference between LN and HN cells when pCO_2 was elevated. Elevated temperature decreased cellular PON content (*t*-test, $t = 6.1$, $df = 4$, $p = 0.004$ for N-replete plus ambient pCO_2 treatment; $t = 5.3$, $df = 4$, $p = 0.006$ for N-replete plus elevated pCO_2 treatment; $t = 3.5$, $df = 4$, $p = 0.023$ for N-limited plus elevated pCO_2 treatment), with the exception of the N-limited plus ambient pCO_2 treatment. A significant interaction between nitrate and pCO_2 levels on PON content was detected (GLM, $F_{1,16} = 34.8$, $p < 0.001$).

While no effects of pCO_2 on C:N were detected under HN conditions, under LN conditions the ratio was decreased or raised by elevated pCO_2 at low or high temperature, respectively (Figure 3a). LN-grown cells showed higher C:N relative to HN-grown cells (*t*-test, $t = -7.1$, $df = 4$, $p = 0.002$ for low temperature plus ambient pCO_2 treatment; $t = -5.6$, $df = 4$, $p = 0.005$ for high temperature plus ambient pCO_2 treatment; $t = -13.8$, $df = 4$, $p < 0.001$ for high temperature plus elevated pCO_2 treatment), with the exception of the low temperature plus elevated pCO_2 treatment. The higher temperature treatment resulted in 76% higher C:N for cells in the N-limited plus elevated pCO_2 treatment (*t*-test, $t = -9.3$, $df = 4$, $p = 0.001$) but had no significant impact on the cells under other treatments. Interactions of the three factors on C:N were detected (Table 3).

Elevated pCO_2 decreased the ratio of cellular BSi to POC (Si:C) by 18–67% (*t*-test, $t = 3.9$, $df = 4$, $p = 0.018$ for low temperature plus N-limited treatment; $t = 3.9$, $df = 4$, $p = 0.017$ for high temperature plus N-replete treatment; $t = 11.6$, $df = 4$, $p < 0.001$ for high temperature plus N-limited treatment; Figure 3b), with the exception of the low temperature plus N-replete treatment. Nitrate limitation increased the Si:C ratio of LC cells and reduced that of HC cells at the elevated temperature (*t*-test, $t = -3.9$, $df = 4$, $p = 0.017$ for LC cells; $t = 8.8$, $df = 4$, $p = 0.001$ for HC cells). The ratio was raised or decreased by elevated temperature at ambient or elevated pCO_2 level under N-limited condition, respectively (*t*-test, $t = -3.2$, $df = 4$, $p = 0.033$ for ambient pCO_2 level; $t = 3.0$, $df = 4$, $p = 0.038$ for elevated pCO_2 level). Interactions between temperature or nitrate and pCO_2 levels on Si:C were detected (Table 3).

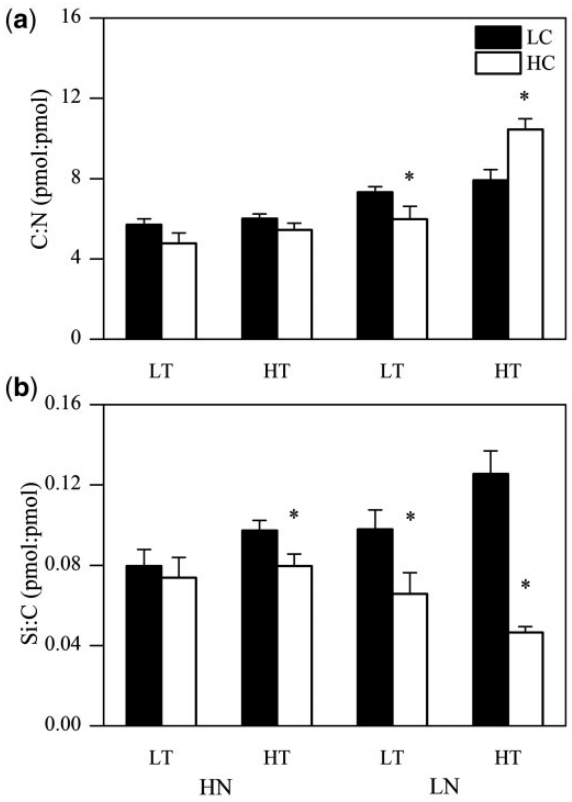

Figure 3. Elemental ratios of POC and PON C:N (pmol:pmol) (a) and ratios of BSi and POC Si:C (pmol:pmol) (b) of *Thalassiosira pseudonana* acclimated to ambient (LC, filled bars) and elevated pCO_2 (HC, open bars) at different temperature and nitrate levels. The data are mean ± *SD* values of triplicate cultures ($n = 3$). Asterisks indicate significant ($p < 0.05$) differences between pCO_2 treatments (*t*-test).

Chlorophyll *a* fluorescence

Nitrate limitation decreased maximal ($\Phi_{PSII\ max}$) and effective ($\Phi_{PSII\ eff}$) photochemical efficiency of PSII (*t*-test, $t = 3.3$, $df = 4$, $p = 0.028$ for $\Phi_{PSII\ max}$ in the low temperature plus ambient pCO_2 treatment; $t = 6.2$, $df = 4$, $p = 0.003$ for $\Phi_{PSII\ max}$ in the low temperature plus elevated pCO_2 treatment; $t = 7.5$, $df = 4$, $p = 0.002$ for $\Phi_{PSII\ max}$ in the high temperature plus ambient pCO_2 treatment; *t*-test, $t = 2.9$, $df = 4$, $p = 0.041$ for $\Phi_{PSII\ eff}$ in the low temperature plus ambient pCO_2 treatment; $t = 5.4$, $df = 4$, $p = 0.006$ for $\Phi_{PSII\ eff}$ in the low temperature plus elevated pCO_2 treatment; $t = 11.1$, $df = 4$, $p < 0.001$ for $\Phi_{PSII\ eff}$ in the high temperature plus ambient pCO_2 treatment; Table 2), with the exception of the high temperature plus ambient pCO_2 treatment. Under N-limited conditions, cells grown at elevated pCO_2 always showed lower $\Phi_{PSII\ max}$ and $\Phi_{PSII\ eff}$ relative to LC cells (*t*-test, $t = 4.2$, $df = 4$, $p = 0.013$ for $\Phi_{PSII\ max}$ at low temperature; $t = 7.5$, $df = 4$, $p = 0.002$ for $\Phi_{PSII\ max}$ at high temperature; *t*-test, $t = 3.2$, $df = 4$, $p = 0.033$ for $\Phi_{PSII\ eff}$ at low temperature; $t = 6.5$, $df = 4$, $p = 0.003$ for $\Phi_{PSII\ eff}$ at high temperature). While elevated pCO_2 did not show effects on the RLCs under HN conditions, it significantly depressed the rETR when nitrate was limiting, especially at high light intensities (Figure 4). Significantly negative effects of elevated pCO_2 on $rETR_{max}$ were detected under N-limited conditions (*t*-test, $t = 4.5$, $df = 4$, $p = 0.011$ for low temperature; $t = 5.2$, $df = 4$, $p = 0.006$ for high temperature). Nitrate limitation significantly decreased $rETR_{max}$ by 14–36% (*t*-test, $t = 6.9$, $df = 4$, $p = 0.002$ for low temperature plus ambient pCO_2 treatment; $t = 10.7$, $df = 4$, $p < 0.001$ for low temperature plus elevated pCO_2 treatment; $t = 4.8$, $df = 4$, $p = 0.009$ for high temperature plus ambient pCO_2 treatment; $t = 7.0$, $df = 4$, $p = 0.002$ for high temperature plus elevated pCO_2 treatment), with a greater decrease at elevated pCO_2 (Table 2). Elevated temperature increased $rETR_{max}$ by 7% in the N-replete plus ambient pCO_2 treatment (*t*-test, $t = -10.7$, $df = 4$, $p < 0.001$), but did not significantly impact the value of this parameter in other treatments. Elevated pCO_2 decreased the apparent light harvesting efficiency (α) at elevated temperature, with a greater decrease under N-limitation (24%, *t*-test, $t = 14.5$, $df = 4$, $p < 0.001$). Elevated temperature significantly enhanced α (*t*-test, $t = -3.0$, $df = 4$, $p = 0.039$ for N-replete plus ambient pCO_2 treatment; $t = -4.0$, $df = 4$, $p = 0.016$ for N-replete plus elevated pCO_2 treatment; $t = -3.4$, $df = 4$, $p = 0.028$ for N-limited plus ambient pCO_2 treatment), with the exception of the N-limited plus elevated pCO_2 treatment. Elevated pCO_2 or temperature showed no effects on the light saturation point (I_k). I_k was 18–27% lower under N-limited conditions compared to HN treatments (*t*-test, $t = 4.4$, $df = 4$, $p = 0.011$ for low temperature plus ambient pCO_2 treatment; $t = 11.8$, $df = 4$, $p < 0.001$ for low temperature plus elevated pCO_2 treatment; $t = 6.9$, $df = 4$, $p = 0.002$ for high temperature plus ambient pCO_2 treatment; $t = 2.8$, $df = 4$, $p = 0.049$ for high temperature plus elevated pCO_2 treatment).

Photosynthetic C fixation and dark respiration

The rate of photosynthetic carbon assimilation was decreased by elevated pCO_2 in LN-grown cells (71%, *t*-test, $t = 29.2$, $df = 4$, $p < 0.001$ for low temperature; 69%, $t = 5.9$, $df = 4$, $p = 0.004$ for high temperature; Figure 5a), but it was unaltered in HN-grown cells. The C fixation rates were 22–89% lower under N-limited conditions compared to N-replete treatments, especially at elevated pCO_2 (*t*-test, $t = 10.4$, $df = 4$, $p < 0.001$ for low temperature plus ambient pCO_2 treatment; $t = 19.2$, $df = 4$, $p < 0.001$ for low temperature plus elevated pCO_2 treatment; $t = 16.3$, $df = 4$, $p < 0.001$ for high temperature plus ambient pCO_2 treatment; $t = 13.4$, $df = 4$, $p < 0.001$ for high temperature plus elevated pCO_2 treatment). An effect of elevated temperature on the carbon fixation rate was only detected in cells at ambient pCO_2: it reduced the rate when nitrate was limiting (*t*-test, $t = 16.1$, $df = 4$, $p < 0.001$), but enhanced the rate under the HN condition (*t*-test, $t = -2.9$, $df = 4$, $p = 0.042$). Interactions between the three factors were detected (Table 3).

While no effects of elevated pCO_2 on respiration were detected in HN treatments, it significantly enhanced the rate under N-limited conditions (Figure 5b). Nitrate limitation increased respiration by 104–303% relative to corresponding HN treatments at elevated pCO_2 level (*t*-test, $t = -9.6$, $df = 4$, $p < 0.001$ for low temperature; $t = -13.1$, $df = 4$, $p < 0.001$ for high temperature). Cells showed enhanced dark respiration rates at higher temperature (GLM, $F_{1,16} = 94.3$, $p < 0.001$), especially under the N-limited plus elevated pCO_2 treatment where respiration was increased by 249% (*t*-test, $t = -17.4$, $df = 4$, $p < 0.001$). Interactions between the three factors were detected (Table 3).

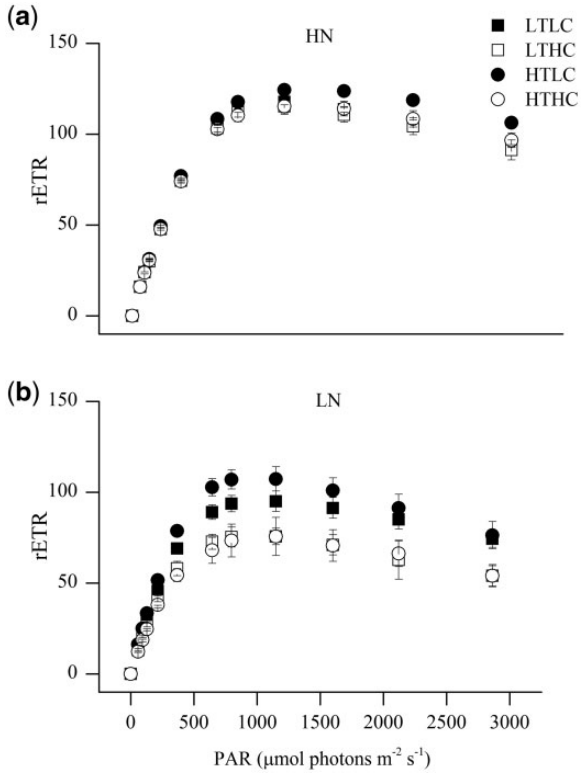

Figure 4. RLCs determined by variations of rETR under a series of light intensities in *Thalassiosira pseudonana* cells at HN (a) and LN (b) levels. The data are means ± *SD* of triplicate cultures ($n = 3$). LTLC, low temperature low pCO_2 treatment; LTHC, low temperature high pCO_2 treatment; HTLC, high temperature low pCO_2 treatment; HTHC, high temperature high pCO_2 treatment.

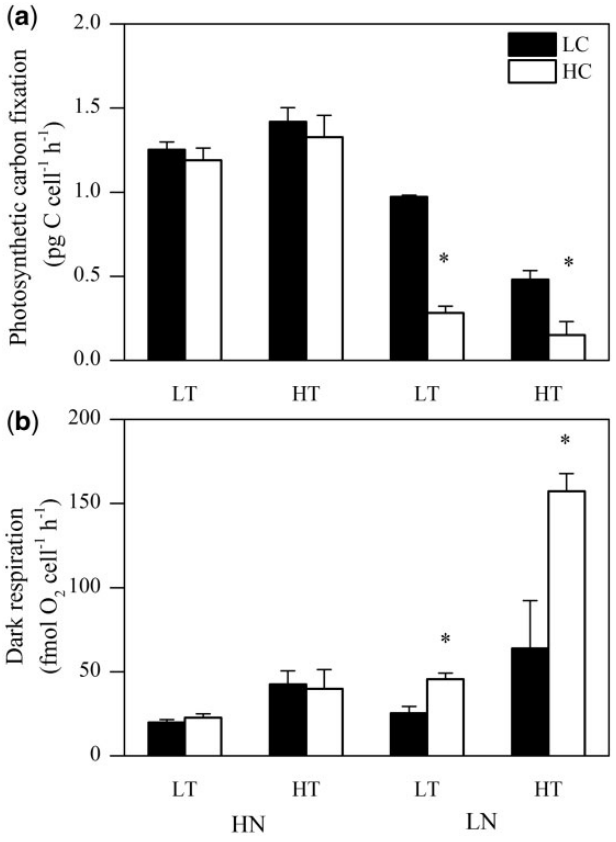

Figure 5. Photosynthetic carbon fixation rates (pg C $cell^{-1}\,h^{-1}$) (a) and dark respiration rates (fmol O_2 $cell^{-1}\,h^{-1}$) (b) of *Thalassiosira pseudonana* acclimated to ambient (LC, filled bars) and elevated pCO_2 (HC, open bars) at different temperature and nitrate levels. The data are mean ± *SD* values of triplicate cultures ($n = 3$). Asterisks indicate significant ($p < 0.05$) differences between pCO_2 treatments (*t*-test).

Discussion

In the present work, *T. pseudonana* showed decreased specific growth rates, cell size, pigment content, photochemical quantum yield of PSII, and photosynthetic carbon fixation under multiple drivers (elevated levels of pCO_2 and temperature and reduced availability of nitrate). Nitrate limitation appeared to act synergistically with elevated pCO_2 and temperature to impact growth and photosynthesis of the diatom. The results imply that a reduction in upward transport of nutrients due to enhanced stratification as a consequence of sea surface warming might reduce growth and carbon fixation by diatoms as ocean acidification progresses.

Effects of elevated temperature and its interaction with nitrate limitation

Elevated temperature, in the present work, decreased the cell size of *T. pseudonana*, which has been suggested to be a general trend in diatoms (Montagnes and Franklin, 2001). Furthermore, higher temperature decreased cellular PON content in *T. pseudonana*, which may be partly correlated with smaller cell size, as indicated by positive relationship between cell size and PON content. The decreased content could also be caused by lowered activity (Gao *et al.*, 2000) and reduced gene expression (Parker and Armbrust, 2005) of nitrate reductase (NR) in diatoms with warming treatments. Down-regulation of nitrogen metabolism by elevated temperature is also supported by observations of declining nitrate uptake rate with increasing temperature in a diatom-dominated phytoplankton community (Lomas and Glibert, 1999). Therefore, negatively affected nitrogen metabolism and enhanced respiration with rising temperature could lead to declining PON and shrinking cell size. This implies a possible slower sinking rate and lower export efficiency of diatoms with ocean warming.

As the major component of photosynthetic architecture, nitrogen could impact the effects of elevated temperature on photosynthesis and growth due to the reduced contents of pigments (Li *et al.*, 2012b) and PSII centres (Berges *et al.*, 1996) and enhanced respiration (Li *et al.*, 2012b) under N-limited conditions. While positive or neutral effects of elevated temperature on specific growth rate, chlorophyll *a* content and photosynthetic carbon fixation rate of *T. pseudonana* cells were detected under N-replete conditions, the warming treatment significantly decreased these parameters under N-limited conditions in the present study. Consistently, the positive effects of elevated temperature on net primary production and phytoplankton biomass were overcompensated by the negative effects of lower nutrient supply due to enhanced stratification associated with ocean warming (Behrenfeld *et al.*, 2006; Lewandowska *et al.*, 2014). Thus, warming could show differential effects on primary production of waters with distinct nutrient conditions.

Effects of elevated CO_2 under nitrate limitation

Higher respiration observed in *T. pseudonana* cells in the N-limited plus elevated CO_2 treatment might be attributed to enhanced glycolytic and tricarboxylic acid cycle pathways under nitrate limitation (Mock *et al.*, 2008; Hockin *et al.*, 2012) and elevated CO_2 conditions (Jin *et al.*, 2015). Enhanced mitochondrial respiration could theoretically lead to increased growth (Geider and Osborne, 1989), as it provides ATP and carbon skeletons for growth (Raven and Beardall, 2005). However, in *T. pseudonana*, the specific growth rate decreased in the nitrogen-limited cells but increased in cells grown under N-replete levels with increased mitochondrial respiration (Figure 6). In other words, negative and positive correlations of specific growth rate and respiration were evident under N-limited and replete conditions, respectively. The photosynthetic light reactions and mitochondrial respiration are two main processes generating ATP in photosynthetic organisms. When the light reactions were repressed under elevated CO_2 and N-limited conditions, mitochondrial respiration could be enhanced to fulfil the cellular energy demand. Although the carbon utilized by mitochondrial respiration must have been initially fixed by photosynthesis, the proportion of fixed carbon for respiration might vary under different conditions. The higher respiration under elevated CO_2 plus N-limited conditions did not, however, result in higher specific growth rate in *T. pseudonana*, which might indicate that the generated energy was allocated more to maintain intracellular homeostasis, rather than growth and biosynthesis. Enhanced (Wu *et al.*, 2010; Yang and Gao, 2012) or unaltered (Trimborn *et al.*, 2014) mitochondrial respiration under seawater acidification conditions have been reported previously in diatoms when nitrogen was replete. In the present work, mitochondrial respiration was substantially enhanced by acidification under N-limited conditions. However, a decreased oxygen uptake rate, determined by the ^{18}O method (Hennon *et al.*, 2014), and reduced expression of the corresponding respiratory gene clusters (Hennon *et al.*, 2015) were reported in *T. pseudonana* grown under seawater acidification ($pH_T = 7.71$) conditions for about 15 generations in a N-limited chemostat. The lack of conformity of effects of acidification on respiration might be caused by differing levels of supplied light energy or light regimes. Continuous light exposure without a dark period, as used in Hennon *et al.* (2014), could have differential effects on mitochondrial respiration relative to a light–dark cycle regime, as shown in *Skeletonema costatum* (Gilstad *et al.*, 1993). Moreover, the inclusion of photorespiration and the Mehler reaction in the oxygen uptake determination in Hennon *et al.* (2014) might also affect the observed changes of mitochondrial respiration to elevated CO_2.

It is worth noting that the decreased chlorophyll content was not the only reason behind the depressed photosynthetic rate per cell at elevated pCO_2 when nitrate was limiting. For instance, under low temperature plus N-limited condition, chlorophyll normalized photosynthesis rates were 0.26 ± 0.02 and 0.11 ± 0.02 μg C (μg chl $a)^{-1}$ h^{-1} for cells at ambient and elevated pCO_2, respectively. While differing effects of nitrogen limitation on the affinity of cells for inorganic carbon and CCMs were observed among species (Raven and Beardall, 2014), nitrogen limitation (Alipanah *et al.*, 2015), and elevated CO_2 (Nakajima *et al.*, 2013; Hennon *et al.*, 2015) could suppress the expression of genes encoding carbonic anhydrases and inorganic carbon transporters, which are essential for uptake and transport of bicarbonate, the predominant dissolved inorganic carbon (DIC) species in seawater, in *T. pseudonana* (Tsuji *et al.*, 2017). Although elevated CO_2 would partly compensate for the decreased bicarbonate uptake, these changes would significantly suppress the DIC uptake and assimilation, as shown by the lowest photosynthetic carbon fixation when nitrate limitation and seawater acidification coexisted (Figure 5a). A decreased number and percentage of active PSII centres of phytoplankton cells were observed under N-limited condition (Berges *et al.*, 1996). Additionally, elevated CO_2 was shown to increase the cost of maintaining functional PSII (McCarthy *et al.*, 2012). However, the demand of nitrogen for repairing inactive PSII could not be fulfilled under N-limited conditions. Thus, lower effective quantum yield of PSII and apparent light harvesting efficiency were observed, which could also contribute to the lowest carbon fixation rate being found under N-limited and elevated CO_2 conditions.

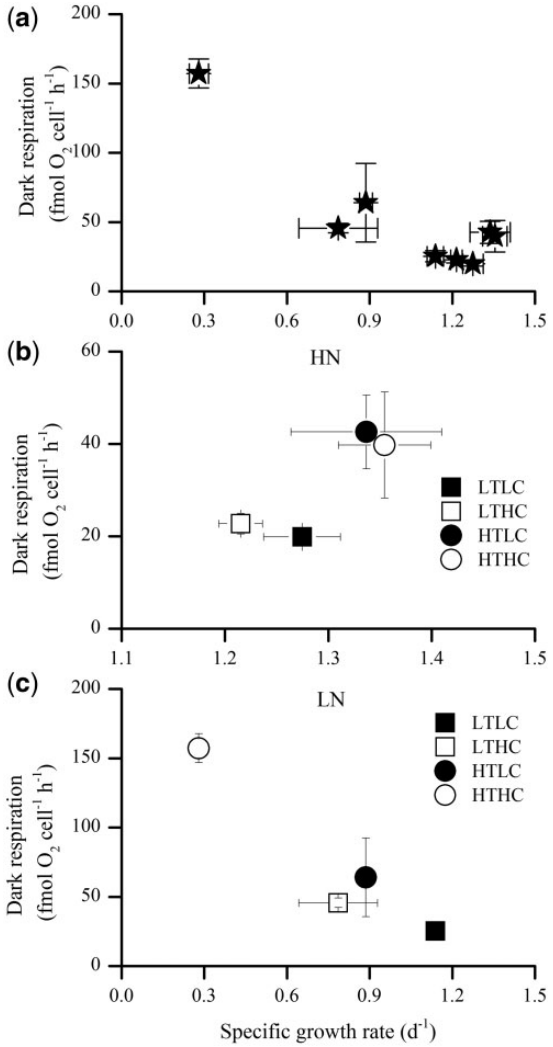

Figure 6. Relationships between dark respiration (fmol O_2 $cell^{-1}$ h^{-1}) and specific growth rates (d^{-1}) of *Thalassiosira pseudonana* cells in eight treatments (a) and the relationships at HN (b) and LN (c) levels. The data are means ± *SD* of triplicate cultures ($n = 3$). LTLC, low temperature low pCO_2 treatment; LTHC, low temperature high pCO_2 treatment; HTLC, high temperature low pCO_2 treatment; HTHC, high temperature high pCO_2 treatment.

Elevated CO_2 and associated seawater chemistry changes usually enhance or do not significantly affect specific growth rate and photosynthesis of *T. pseudonana* (strain CCMP 1335) under nitrogen-replete conditions (Figure 7). However, in the present work, under nitrate limitation, the acidification treatment markedly impacted its physiological performance. As the two main electron sinks (Giordano and Raven, 2014), carbon and nitrogen assimilation processes compete for energy and reductant in photosynthetic organisms (Huppe and Turpin, 1994). Diatoms have evolved vacuoles to store nutrients (Falkowski *et al.*, 2004), which enables cells to optimize carbon and nitrogen assimilation by reallocating energy and reductant when light is optimal and other resources are abundant. These characteristics could allow cells to maintain constant or higher growth and photosynthesis under seawater acidification. When nitrogen is limited, energy and reductant pools markedly decreased as photosynthetic capacity decreased. However, expressions of genes encoding nitrogen transport and metabolism (NR and NADPH-dependent nitrite reductase) were up-regulated under N-limited conditions, indicating the up-regulation of nitrogen metabolism (Alipanah *et al.*, 2015). Elevated CO_2 and associated seawater acidification, although saving some of the energy used for CCMs (Hopkinson *et al.*, 2011), add an additional energy burden to cells to maintain intracellular pH homeostasis through adjusting cellular periplasmic redox activity and/or proton pumping (Taylor *et al.*, 2012). Thus, elevated CO_2 under N-limited conditions could impact the physiological performance of photosynthetic cells as clearly shown in the present study. Moreover, addition of a warming treatment exacerbated the negative effects of acidification on specific growth rate and chlorophyll content under the N-limited conditions (Figure 1a and 2a). The mechanism underpinning these changes might be that elevated temperature could increase the nitrogen to phosphate ratio of *T. pseudonana* (Toseland *et al.*, 2013), which would increase cellular demand for nitrogen and intensify the nitrogen limitation on cells under the low N conditions.

Interactions of elevated CO_2 with other abiotic factors

The effects of elevated CO_2 on phytoplankton might be closely related to changes of other factors, as the organismal energy budget can be altered under a range of stress conditions (Wingler *et al.*, 2000). Under optimal conditions, the effects of CO_2 might be overshadowed by other factors, such as light, nutrient supply, and temperature (Boyd *et al.*, 2010). However, the effects of elevated CO_2 and associated seawater acidification tend to be more conspicuous when other factors are limiting or stressful. For instance, negative effects of acidification on growth of diatoms were detected under high levels of solar radiation (Gao *et al.*, 2012b), low light, and low temperature (Passow and Laws, 2015) and in the presence of solar UV radiation (Li *et al.*, 2017a). Recently, a depressed maximum quantum yield of PSII in *T. pseudonana* under acidification was found to occur only when nitrogen availability was reduced (in stationary phase) (Hong *et al.*, 2017). Nevertheless, elevated CO_2 and associated seawater acidification might also show more prominent effects on diatoms under nutrient-replete conditions relative to limited conditions, as documented in studies on *T. weissflogii* (Sugie and Yoshimura, 2016) and *P. tricornutum* (Li *et al.*, 2012b). An increasing number of environmental factors could influence the effects of elevated CO_2 on microalgae (Brennan and Collins, 2015), which is also shown in this study on the diatom *T. pseudonana*.

Effects of the three factors on elemental ratios

Changes in diatom elemental stoichiometry and macromolecular composition can impact predation by, and reproduction of, zooplankton (Elser *et al.*, 2000; Wichard *et al.*, 2007) and export of particulate organic matter to deep waters. In *T. pseudonana*, C:N was differentially impacted by elevated CO_2 at low and high temperatures under nitrogen limitation (Figure 3), which resulted from variations in cellular POC and PON under elevated CO_2 conditions at different temperatures. The higher C:N indicates a lower nutritional quality of phytoplankton as prey for higher trophic levels (Elser *et al.*, 2000). The decreased Si:C at elevated CO_2 under nitrogen limitation (Figure 3) was mainly due to increased POC. Decreased Si:C with seawater acidification has also been shown in other diatom species (Tatters *et al.*, 2012; Mejia *et al.*, 2013; Li *et al.*, 2016). Interactions of acidification, N-limitation, and warming appear to give rise to reduced ratios of silicate per carbon. BSi contents were constant among treatments; thus, the ballasting effects by diatom frustules might not change. Nevertheless, the decreased Si:C would modify the primary production contributed by diatom communities and local carbon and silicon budgets in Si-limited waters (Mejia *et al.*, 2013).

Conclusions

The present study emphasizes the importance of investigating effects of elevated CO_2 under changes of other drivers. Until now, effects of seawater acidification on diatoms have been extensively studied under nitrogen-replete conditions (Gao and Campbell, 2014 and references therein). However, contrasting effects of acidification on *T. pseudonana* were detected under nitrate-limited and replete conditions (Figure 7), which indicates that elevated CO_2 could show distinct effects on phytoplankton living in waters with different nutritional conditions. Moreover, the present study highlights the critical role of nitrogen availability in influencing the effects of seawater acidification and elevated sea surface temperatures on growth and photosynthesis in diatoms. Positive or neutral effects of acidification and warming on growth and photosynthesis of diatoms under nutrient replete conditions (Montagnes and Franklin, 2001; Kroeker *et al.*, 2013) might be reversed to negative impacts when cells are nutrient-limited. *T. pseudonana* cells showed the lowest specific growth rate and photosynthetic carbon fixation rate under the combined conditions of elevated temperature, N-limitation, and seawater acidification, which is the scenario predicted for future oceanic ecosystems (Boyd *et al.*, 2015). Thus, the negative effects of ocean warming on net primary production and phytoplankton biomass of low- and mid-latitude oceans (Behrenfeld *et al.*, 2006; Boyce *et al.*, 2010) could be further exacerbated under future ocean conditions. As the indispensable base and component of marine food webs, diatoms might be negatively impacted by changes of oceanic environmental factors. Hence, the base of marine food webs and the strength of the biological CO_2 pump could be impacted severely by future CO_2-induced seawater acidification and elevated temperature in a way that is also dependent on the nutritional conditions of local waters. However, it should be noticed that the responses of diatoms to seawater acidification might depend on the timescale over which they are exposed as longer term exposure to changed conditions leads to different

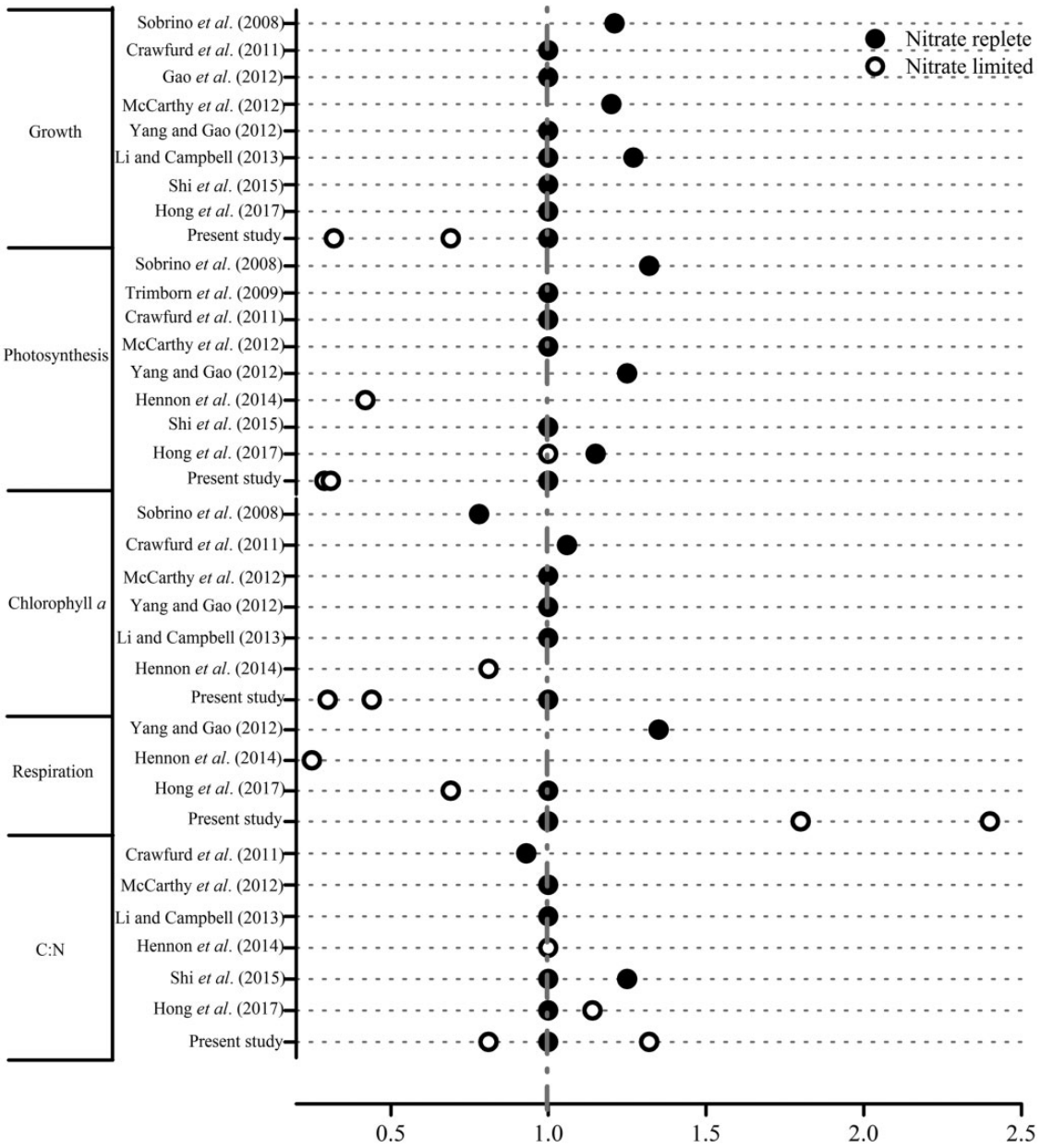

Figure 7. Impact of seawater acidification on physiological parameters of *Thalassiosira pseudonana* (strain CCMP 1335) cells. Data are the fold difference of means of these parameters at elevated pCO_2 level (HC) compared to means at ambient pCO_2 level (LC), i.e. the ratios of HC to LC. Filled and open circles show the ratios under replete and limited nitrate conditions respectively.

physiological responses (Li *et al.*, 2017b), and therefore caution should be exercised in directly extrapolating the results obtained from relatively short-term studies to the long-term ocean acidification process.

Data availability

Data in the present study are available at https://doi.pangaea.de/10.1594/PANGAEA.880576.

Acknowledgements

The authors would like to thank the two anonymous reviewers and the editor for their insightful comments on the manuscript. This study was supported by National Natural Science Foundation of China (41430967, 41720104005, 41721005) and Joint project of National Natural Science Foundation of China and Shandong province (No. U1606404). JB's visit to Xiamen was supported by Xiamen University.

References

Agusti, S., González-Gordillo, J. I., Vaqué, D., Estrada, M., Cerezo, M. I., Salazar, G., Gasol, J. M. et al. 2015. Ubiquitous healthy diatoms in the deep sea confirm deep carbon injection by the biological pump. Nature Communications 6: 7608.

Alipanah, L., Rohloff, J., Winge, P., Bones, A. M., and Brembu, T. 2015. Whole-cell response to nitrogen deprivation in the diatom *Phaeodactylum tricornutum*. Journal of Experimental Botany 66: 6281–6296.

Araújo, S. C., and Garcia, V. M. T. 2005. Growth and biochemical composition of the diatom *Chaetoceros cf. wighamii* brightwell under different temperature, salinity and carbon dioxide levels. I. Protein, carbohydrates and lipids. Aquaculture 246: 405–412.

Beardall, J., Stojkovic, S., and Larsen, S. 2009. Living in a high CO_2 world: impacts of global climate change on marine phytoplankton. Plant Ecology & Diversity 2: 191–205.

Beardall, J., Stojkovic, S., and Gao, K. 2014. Interactive effects of nutrient supply and other environmental factors on the sensitivity of marine primary producers to ultraviolet radiation: implications for the impacts of global change. Aquatic Biology 22: 5–23.

Behrenfeld, M. J., O'Malley, R. T., Siegel, D. A., McClain, C. R., Sarmiento, J. L., Feldman, G. C., Milligan, A. J. et al. 2006. Climate-driven trends in contemporary ocean productivity. Nature 444: 752–755.

Beman, J. M., Chow, C.-E., King, A. L., Feng, Y., Fuhrman, J. A., Andersson, A., Bates, N. R. et al. 2011. Global declines in oceanic nitrification rates as a consequence of ocean acidification. Proceedings of the National Academy of Sciences of the United States of America 108: 208–213.

Berges, J. A., Charlebois, D. O., Mauzerall, D. C., and Falkowski, P. G. 1996. Differential effects of nitrogen limitation on photosynthetic efficiency of photosystems I and II in microalgae. Plant Physiology 110: 689–696.

Bopp, L., Resplandy, L., Orr, J. C., Doney, S. C., Dunne, J. P., Gehlen, M., Halloran, P. et al. 2013. Multiple stressors of ocean ecosystems in the 21st century: projections with CMIP5 models. Biogeosciences 10: 6225–6245.

Boyce, D. G., Lewis, M. R., and Worm, B. 2010. Global phytoplankton decline over the past century. Nature 466: 591–596.

Boyd, P. W., Strzepek, R., Fu, F., and Hutchins, D. A. 2010. Environmental control of open-ocean phytoplankton groups: now and in the future. Limnology and Oceanography 55: 1353–1376.

Boyd, P. W., Rynearson, T. A., Armstrong, E. A., Fu, F., Hayashi, K., Hu, Z., Hutchins, D. A. et al. 2013. Marine phytoplankton temperature versus growth responses from polar to tropical waters – outcome of a scientific community-wide study. PLoS One 8: e63091.

Boyd, P. W., Lennartz, S. T., Glover, D. M., and Doney, S. C. 2015. Biological ramifications of climate-change-mediated oceanic multi-stressors. Nature Climate Change 5: 71–79.

Boyd, P. W., Cornwall, C. E., Davison, A., Doney, S. C., Fourquez, M., Hurd, C. L., Lima, I. D. et al. 2016. Biological responses to environmental heterogeneity under future ocean conditions. Global Change Biology 22: 2633–2650.

Brennan, G., and Collins, S. 2015. Growth responses of a green alga to multiple environmental drivers. Nature Climate Change 5: 892–897.

Brzezinski, M. A., and Nelson, D. M. 1995. The annual silica cycle in the Sargasso Sea near Bermuda. Deep Sea Research Part I: Oceanographic Research Papers 42: 1215–1237.

Coello-Camba, A., Agustí, S., Holding, J., Arrieta, J. M., and Duarte, C. M. 2014. Interactive effect of temperature and CO_2 increase in Arctic phytoplankton. Frontiers in Marine Science 1: 49.

Collins, S., Rost, B., and Rynearson, T. A. 2014. Evolutionary potential of marine phytoplankton under ocean acidification. Evolutionary Applications 7: 140–155.

Crawfurd, K. J., Raven, J. A., Wheeler, G. L., Baxter, E. J., and Joint, I. 2011. The response of *Thalassiosira pseudonana* to long-term exposure to increased CO_2 and decreased pH. PLoS One 6: e26695.

Doyle, S. A., Saros, J. E., and Williamson, C. E. 2005. Interactive effects of temperature and nutrient limitation on the response of alpine phytoplankton growth to ultraviolet radiation. Limnology and Oceanography 50: 1362–1367.

Eilers, P., and Peeters, J. 1988. A model for the relationship between light intensity and the rate of photosynthesis in phytoplankton. Ecological Modelling 42: 199–215.

Elser, J. J., Fagan, W. F., Denno, R. F., Dobberfuhl, D. R., Folarin, A., Huberty, A., Interlandi, S. et al. 2000. Nutritional constraints in terrestrial and freshwater food webs. Nature 408: 578–580.

Eppley, R. W., Rogers, J. N., and McCarthy, J. J. 1969. Half-saturation constants for uptake of nitrate and ammonium by marine phytoplankton. Limnology and Oceanography 14: 912–920.

Falkowski, P. G. 1975. Nitrate uptake in marine phytoplankton: comparison of half-saturation constants from seven species. Limnology and Oceanography 20: 412–417.

Falkowski, P. G., Katz, M. E., Knoll, A. H., Quigg, A., Raven, J. A., Schofield, O., and Taylor, F. 2004. The evolution of modern eukaryotic phytoplankton. Science 305: 354–360.

Feng, Y., Hare, C. E., Leblanc, K., Rose, J. M., Zhang, Y., DiTullio, G. R., Lee, P. et al. 2009. Effects of increased pCO_2 and temperature on the North Atlantic Spring Bloom: I. The phytoplankton community and biogeochemical response. Marine Ecology Progress Series 388: 13–25.

Gao, Y., Smith, G. J., and Alberte, R. S. 2000. Temperature dependence of nitrate reductase activity in marine phytoplankton: biochemical analysis and ecological implications. Journal of Phycology 36: 304–313.

Gao, K., Wu, Y., Li, G., Wu, H., Villafane, V. E., and Helbling, E. W. 2007. Solar UV radiation drives CO_2 fixation in marine phytoplankton: a double-edged sword. Plant Physiology 144: 54–59.

Gao, K., Helbling, E. W., Häder, D. P., and Hutchins, D. A. 2012a. Responses of marine primary producers to interactions between ocean acidification, solar radiation, and warming. Marine Ecology Progress Series 470: 167–189.

Gao, K., Xu, J., Gao, G., Li, Y., Hutchins, D. A., Huang, B., Wang, L. et al. 2012b. Rising CO_2 and increased light exposure synergistically reduce marine primary productivity. Nature Climate Change 2: 519–523.

Gao, K., and Campbell, D. A. 2014. Photophysiological responses of marine diatoms to elevated CO_2 and decreased pH: a review. Functional Plant Biology 41: 449–459.

Gattuso, J.-P., Magnan, A., Bille, R., Cheung, W. W. L., Howes, E. L., Joos, F., Allemand, D. et al. 2015. Contrasting futures for ocean and society from different anthropogenic CO_2 emissions scenarios. Science 349: aac4722.

Geider, R. J., and Osborne, B. A. 1989. Respiration and microalgal growth: a review of the quantitative relationship between dark respiration and growth. New Phytologist 112: 327–341.

Gilstad, M., Johnsen, G., and Sakshaug, E. 1993. Photosynthetic parameters, pigment composition and respiration rates of the marine diatom *Skeletonema costatum* grown in continuous light and a 12: 12 h light-dark cycle. Journal of Plankton Research 15: 939–951.

Giordano, M., and Raven, J. A. 2014. Nitrogen and sulfur assimilation in plants and algae. Aquatic Botany 118: 45–61.

Hagerthey, S. E., Defew, E. C., and Paterson, D. M. 2002. Influence of *Corophium volutator* and *Hydrobia ulvae* on intertidal benthic diatom assemblages under different nutrient and temperature regimes. Marine Ecology Progress Series 245: 47–59.

Halsey, K. H., Milligan, A. J., and Behrenfeld, M. J. 2011. Linking time-dependent carbon-fixation efficiencies in *Dunaliella tertiolecta* (Chlorophyceae) to underlying metabolic pathways. Journal of Phycology 47: 66–76.

Halsey, K. H., O'Malley, R. T., Graff, J. R., Milligan, A. J., and Behrenfeld, M. J. 2013. A common partitioning strategy for photosynthetic products in evolutionarily distinct phytoplankton species. New Phytologist 198: 1030–1038.

Heiden, J. P., Bischof, K., and Trimborn, S. 2016. Light intensity modulates the response of two Antarctic diatom species to ocean acidification. Frontiers in Marine Science 3: 260.

Hennon, G. M. M., Quay, P., Morales, R. L., Swanson, L. M., and Virginia Armbrust, E. 2014. Acclimation conditions modify physiological response of the diatom *Thalassiosira pseudonana* to elevated CO_2 concentrations in a nitrate-limited chemostat. Journal of Phycology 50: 243–253.

Hennon, G. M. M., Ashworth, J., Groussman, R. D., Berthiaume, C., Morales, R. L., Baliga, N. S., Orellana, M. V. et al. 2015. Diatom acclimation to elevated CO_2 via cAMP signalling and coordinated gene expression. Nature Climate Change 5: 761–765.

Hockin, N. L., Mock, T., Mulholland, F., Kopriva, S., and Malin, G. 2012. The response of diatom central carbon metabolism to nitrogen starvation is different from that of green algae and higher plants. Plant Physiology 158: 299–312.

Hong, H., Li, D., Lin, W., Li, W., and Shi, D. 2017. Nitrogen nutritional condition affects the response of energy metabolism in diatoms to elevated carbon dioxide. Marine Ecology Progress Series 567: 41–56.

Hopkinson, B. M., Dupont, C. L., Allen, A. E., and Morel, F. M. 2011. Efficiency of the CO_2-concentrating mechanism of diatoms. Proceedings of the National Academy of Sciences of the United States of America 108: 3830–3837.

Hoppe, C. J., Holtz, L. M., Trimborn, S., and Rost, B. 2015. Ocean acidification decreases the light-use efficiency in an Antarctic diatom under dynamic but not constant light. New Phytologist 207: 159–171.

Huppe, H., and Turpin, D. 1994. Integration of carbon and nitrogen metabolism in plant and algal cells. Annual Review of Plant Biology 45: 577–607.

Jin, P., Wang, T., Liu, N., Dupont, S., Beardall, J., Boyd, P. W., Riebesell, U. et al. 2015. Ocean acidification increases the accumulation of toxic phenolic compounds across trophic levels. Nature Communications 6: 8714.

King, A. L., Sanudo-Wilhelmy, S. A., Leblanc, K., Hutchins, D. A., and Fu, F. 2011. CO_2 and vitamin B_{12} interactions determine bioactive trace metal requirements of a subarctic Pacific diatom. The ISME Jornal 5: 1388–1396.

King, A. L., Jenkins, B. D., Wallace, J. R., Liu, Y., Wikfors, G. H., Milke, L. M., and Meseck, S. L. 2015. Effects of CO_2 on growth rate, C: N: P, and fatty acid composition of seven marine phytoplankton species. Marine Ecology Progress Series 537: 59–69.

Kroeker, K. J., Kordas, R. L., Crim, R., Hendriks, I. E., Ramajo, L., Singh, G. S., Duarte, C. M. et al. 2013. Impacts of ocean acidification on marine organisms: quantifying sensitivities and interaction with warming. Global Change Biology 19: 1884–1896.

Langer, G., Geisen, M., Baumann, K. H., Kläs, J., Riebesell, U., Thoms, S., and Young, J. R. 2006. Species-specific responses of calcifying algae to changing seawater carbonate chemistry. Geochemistry, Geophysics, Geosystems 7: Q09006.

Langer, G., Nehrke, G., Probert, I., Ly, J., and Ziveri, P. 2009. Strain-specific responses of *Emiliania huxleyi* to changing seawater carbonate chemistry. Biogeosciences 6: 2637–2646.

Lewandowska, A. M., Boyce, D. G., Hofmann, M., Matthiessen, B., Sommer, U., and Worm, B. 2014. Effects of sea surface warming on marine plankton. Ecology Letters 17: 614–623.

Li, F., Wu, Y., Hutchins, D. A., Fu, F., and Gao, K. 2016. Physiological responses of coastal and oceanic diatoms to diurnal fluctuations in seawater carbonate chemistry under two CO_2 concentrations. Biogeosciences 13: 6247–6259.

Li, F., Beardall, J., Collins, S., and Gao, K. 2017b. Decreased photosynthesis and growth with reduced respiration in the model diatom *Phaeodactylum tricornutum* grown under elevated CO_2 over 1800 generations. Global Change Biology 23: 127–137.

Li, W., Gao, K., and Beardall, J. 2012b. Interactive effects of ocean acidification and nitrogen-limitation on the diatom *Phaeodactylum tricornutum*. PLoS One 7: e51590.

Li, W., Yang, Y., Li, Z., Xu, J., and Gao, K. 2017a. Effects of seawater acidification on the growth rates of the diatom *Thalassiosira (Conticribra) weissflogii* under different nutrient, light, and UV radiation regimes. Journal of Applied Phycology 29: 133–142.

Li, Y., Gao, K., Villafañe, V. E., and Helbling, E. W. 2012a. Ocean acidification mediates photosynthetic response to UV radiation and temperature increase in the diatom *Phaeodactylum tricornutum*. Biogeosciences 9: 3931–3942.

Li, Y., Xu, J., and Gao, K. 2014. Light-modulated responses of growth and photosynthetic performance to ocean acidification in the model diatom *Phaeodactylum tricornutum*. PLoS One 9: e96173.

Liu, N., Beardall, J., and Gao, K. 2017. Elevated CO_2 and associated seawater chemistry do not benefit a model diatom grown with increased availability of light. Aquatic Microbial Ecology 79: 137–147.

Lomas, M. W., and Glibert, P. M. 1999. Temperature regulation of nitrate uptake: a novel hypothesis about nitrate uptake and reduction in cool-water diatoms. Limnology and Oceanography 44: 556–572.

McCarthy, A., Rogers, S. P., Duffy, S. J., and Campbell, D. A. 2012. Elevated carbon dioxide differentially alters the photophysiology of *Thalassiosira pseudonana* (Bacillariophyceae) and *Emiliania huxleyi* (Haptophyta). Journal of Phycology 48: 635–646.

Mejia, L. M., Isensee, K., Méndez-Vicente, A., Pisonero, J., Shimizu, N., González, C., and Monteleone, B. 2013. B content and Si/C ratios from cultured diatoms (*Thalassiosira pseudonana* and *Thalassiosira weissflogii*): relationship to seawater pH and diatom carbon acquisition. Geochimica Et Cosmochimica Acta 123: 322–337.

Mock, T., Samanta, M. P., Iverson, V., Berthiaume, C., Robison, M., Holtermann, K., Durkin, C. et al. 2008. Whole-genome expression profiling of the marine diatom *Thalassiosira pseudonana* identifies genes involved in silicon bioprocesses. Proceedings of the National Academy of Sciences of the United States of America 105: 1579–1584.

Montagnes, D. J., and Franklin, M. 2001. Effect of temperature on diatom volume, growth rate, and carbon and nitrogen content: reconsidering some paradigms. Limnology and Oceanography 46: 2008–2018.

Moore, J. K., Doney, S. C., Kleypas, J. A., Glover, D. M., and Fung, I. Y. 2002a. An intermediate complexity marine ecosystem model for the global domain. Deep Sea Research Part II: Topical Studies in Oceanography 49: 403–462.

Moore, J. K., Doney, S. C., Glover, D. M., and Fung, I. Y. 2002b. Iron cycling and nutrient-limitation patterns in surface waters of the World Ocean. Deep Sea Research Part II: Topical Studies in Oceanography 49: 463–507.

Nakajima, K., Tanaka, A., and Matsuda, Y. 2013. SLC4 family transporters in a marine diatom directly pump bicarbonate from seawater. Proceedings of the National Academy of Sciences of the United States of America 110: 1767–1772.

Parker, M. S., and Armbrust, E. V. 2005. Synergistic effects of light, temperature, and nitrogen source on transcription of genes for carbon and nitrogen metabolism in the centric diatom *Thalassiosira pseudonana* (Bacillariophyceae). Journal of Phycology 41: 1142–1153.

Passow, U., and Laws, E. A. 2015. Ocean acidification as one of multiple stressors: growth response of *Thalassiosira weissflogii* (diatom) under temperature and light stress. Marine Ecology Progress Series 541: 75–90.

Raven, J. A., and Beardall, J. 2005. Respiration in aquatic photolithotrophs. *In* Respiration in Aquatic Ecosystems, pp. 36–46. Ed. by P. A. del Giorgio and P. J. le B. Williams. Oxford University Press, New York. 315 pp.

Raven, J. A., and Beardall, J. 2014. CO_2 concentrating mechanisms and environmental change. Aquatic Botany 118: 24–37.

Ritchie, R. J. 2006. Consistent sets of spectrophotometric chlorophyll equations for acetone, methanol and ethanol solvents. Photosynthesis Research 89: 27–41.

Rost, B., Zondervan, I., and Wolf-Gladrow, D. 2008. Sensitivity of phytoplankton to future changes in ocean carbonate chemistry: current knowledge, contradictions and research directions. Marine Ecology Progress Series 373: 227–237.

Segovia, M., Lorenzo, M. R., Maldonado, M. T., Larsen, A., Berger, S. A., Tsagaraki, T. M., Lázaro, F. J. et al. 2017. Iron availability modulates the effects of future CO_2 levels within the marine planktonic food web. Marine Ecology Progress Series 565: 17–33.

Shi, D., Li, W., Hopkinson, B. M., Hong, H., Li, D., Kao, S.-J., and Lin, W. 2015. Interactive effects of light, nitrogen source, and carbon dioxide on energy metabolism in the diatom *Thalassiosira pseudonana*. Limnology and Oceanography 60: 1805–1822.

Sobrino, C., Ward, M. L., and Neale, P. J. 2008. Acclimation to elevated carbon dioxide and ultraviolet radiation in the diatom *Thalassiosira pseudonana*: effects on growth, photosynthesis, and spectral sensitivity of photoinhibition. Limnology and Oceanography 53: 494–505.

Suffrian, K., Schulz, K. G., Gutowska, M. A., Riebesell, U., and Bleich, M. 2011. Cellular pH measurements in *Emiliania huxleyi* reveal pronounced membrane proton permeability. New Phytologist 190: 595–608.

Sugie, K., and Yoshimura, T. 2013. Effects of pCO_2 and iron on the elemental composition and cell geometry of the marine diatom *Pseudo-nitzschia pseudodelicatissima* (Bacillariophyceae). Journal of Phycology 49: 475–488.

Sugie, K., and Yoshimura, T. 2016. Effects of high CO_2 levels on the ecophysiology of the diatom *Thalassiosira weissflogii* differ depending on the iron nutritional status. ICES Journal of Marine Science 73: 680–692.

Sun, J., Hutchins, D. A., Feng, Y., Seubert, E. L., Caron, D. A., and Fu, F. 2011. Effects of changing pCO_2 and phosphate availability on domoic acid production and physiology of the marine harmful bloom diatom *Pseudo-nitzschia multiseries*. Limnology and Oceanography 56: 829–840.

Sunda, W. G., Price, N. M., and Morel, F. M. 2005. Trace metal ion buffers and their use in culture studies. *In* Algal Culturing Techniques, pp. 35–63. Ed. by R. A. Aderson. Elsevier Academic Press, Burlington. 578 pp.

Tatters, A. O., Fu, F.-X., Hutchins, D. A., and Neilan, B. 2012. High CO_2 and silicate limitation synergistically increase the toxicity of *Pseudo-nitzschia fraudulenta*. PLoS One 7: e32116.

Tatters, A. O., Roleda, M. Y., Schnetzer, A., Fu, F., Hurd, C. L., Boyd, P. W., Caron, D. A. et al. 2013. Short- and long-term conditioning of a temperate marine diatom community to acidification and warming. Philosophical Transactions of the Royal Society B: Biological Sciences 368: 20120437.

Taucher, J., Jones, J., James, A., Brzezinski, M. A., Carlson, C. A., Riebesell, U., and Passow, U. 2015. Combined effects of CO_2 and temperature on carbon uptake and partitioning by the marine diatoms *Thalassiosira weissflogii* and *Dactyliosolen fragilissimus*. Limnology and Oceanography 60: 901–919.

Taylor, A. R., Brownlee, C., and Wheeler, G. L. 2012. Proton channels in algae: reasons to be excited. Trends in Plant Science 17: 675–684.

Torstensson, A., Chierici, M., and Wulff, A. 2012. The influence of increased temperature and carbon dioxide levels on the benthic/-sea ice diatom *Navicula directa*. Polar Biology 35: 205–214.

Torstensson, A., Hedblom, M., Andersson, J., Andersson, M. X., and Wulff, A. 2013. Synergism between elevated pCO_2 and temperature on the Antarctic sea ice diatom *Nitzschia lecointei*. Biogeosciences 10: 6391–6401.

Toseland, A., Daines, S. J., Clark, J. R., Kirkham, A., Strauss, J., Uhlig, C., Lenton, T. M. et al. 2013. The impact of temperature on marine phytoplankton resource allocation and metabolism. Nature Climate Change 3: 979–984.

Trimborn, S., Wolf-Gladrow, D., Richter, K.-U., and Rost, B. 2009. The effect of pCO_2 on carbon acquisition and intracellular assimilation in four marine diatoms. Journal of Experimental Marine Biology and Ecology 376: 26–36.

Trimborn, S., Thoms, S., Petrou, K., Kranz, S. A., and Rost, B. 2014. Photophysiological responses of Southern Ocean phytoplankton to changes in CO_2 concentrations: short-term versus acclimation effects. Journal of Experimental Marine Biology and Ecology 451: 44–54.

Tsuji, Y., Mahardika, A., and Matsuda, Y. 2017. Evolutionarily distinct strategies for the acquisition of inorganic carbon from seawater in marine diatoms. Journal of Experimental Botany doi: 10.1093/jxb/erx102.

Verspagen, J. M. H., Van de Waal, D. B., Finke, J. F., Visser, P. M., and Huisman, J. 2014. Contrasting effects of rising CO_2 on primary production and ecological stoichiometry at different nutrient levels. Ecology Letters 17: 951–960.

Wichard, T., Gerecht, A., Boersma, M., Poulet, S. A., Wiltshire, K., and Pohnert, G. 2007. Lipid and fatty acid composition of diatoms revisited: rapid wound-activated change of food quality parameters influences herbivorous copepod reproductive success. ChemBioChem 8: 1146–1153.

Williams, P. J., Le B., Thomas, D. N., and., and Reynolds, C. S. 2002. Phytoplankton Productivity: Carbon Assimilation in Marine and Freshwater Ecology. Wiley-Blackwell, Oxford. 400 pp.

Wingler, A., Lea, P. J., Quick, W. P., and Leegood, R. C. 2000. Photorespiration: metabolic pathways and their role in stress protection. Philosophical Transactions of the Royal Society of London. Series B: Biological Sciences 355: 1517–1529.

Wu, Y., Gao, K., and Riebesell, U. 2010. CO_2-induced seawater acidification affects physiological performance of the marine diatom *Phaeodactylum tricornutum*. Biogeosciences 7: 2915–2923.

Yang, G., and Gao, K. 2012. Physiological responses of the marine diatom *Thalassiosira pseudonana* to increased pCO_2 and seawater acidity. Marine Environmental Research 79: 142–151.

Handling editor: Shubha Sathyendranath